

Designing Small Propellers for Optimum Efficiency and Low Noise Footprint

Charles F. Wisniewski,^{*} Aaron R. Byerley,[†] and William H. Heiser[‡]
USAF Academy, CO, 80132

Kenneth W. Van Treuren[§] and William R. Liller, III^{**}
Baylor University, Waco, TX, 76798

A topic of increasing importance in the Unmanned Aerial System (UAS) community is the design and performance of open propellers used in hand launched, small UASs. The design and testing of these propellers is necessary to accurately predict UAS operation. This paper describes the design methodology used by Baylor University and the USAF Academy to design propeller blades for optimum efficiency and low noise. Propeller blade design theories are discussed as well as an overview of several of the existing design codes. Included is a discussion on geometric angle of attack, the induced angle of attack, and their impact on propeller design. The design program BEARCONTROL was developed which incorporates the programs QMIL and QPROP. Supplemental codes were also developed to work with Bearcontrol to design a propeller with a constant chord and variable twist. This resulted in the angle of attack for L/D_{\max} being used from the propeller hub to the tip. BEARCONTROL is a program written in MATLAB that gives a user the ability to quickly design a propeller, predict its performance, and then create a 3D model in SolidWorks. The MATLAB GUI ultimately results in a mostly automated process that is simple to use for individuals who are unfamiliar with command prompt programs and SolidWorks modeling. Also incorporated into BEARCONTROL is the program NREL AirFoil Noise (NAFNOISE) developed by the National Renewable Energy Laboratory (NREL). This program predicts the noise of any airfoil shape and provides a comparison for optimizing/minimizing predicted noise for the propeller being designed. Construction methods and materials also have a direct impact on cost, durability and operability when using a rapid prototype process to fabricate propellers. An overview of materials and construction methods used in this research are discussed. Incorporation of a hub with interchangeable blades is also presented as a more efficient testing method.

Nomenclature

A	=	throughflow area (perpendicular to the station local velocity), in^2
B	=	number of blades
$BEMT$	=	Blade Element Momentum Theory
BET	=	Blade Element Theory
c	=	chord
c_d	=	blade section drag coefficient
c_l	=	blade section lift coefficient
D	=	propeller outer diameter, in , propeller blade drag, lb_f
F	=	thrust force
L	=	lift, lb_f
n	=	number of propeller blades, rotational velocity in cycles per second
p	=	static pressure, lb_f/ft^2

^{*} Propulsion Research Associate, Department of Aeronautics, USAF Academy, and Senior Member.

[†] Professor, Department of Aeronautics, USAF Academy, and Senior Member.

[‡] Professor Emeritus, Department of Aeronautics, USAF Academy, and Honorary Fellow.

[§] Professor, Department of Mechanical Engineering, Baylor University #97356, and Senior Member.

^{**} Graduate Student, Department of Mechanical Engineering, Baylor University #97356, and Student Member.

Q	= torque, $ft\ lb_f$
r	= arbitrary radius, in
RPM	= rotational speed, <i>revolutions per minute</i>
R	= propeller outer radius, in
Re	= Reynolds number
SPL	= sound pressure level, dB
T	= propeller thrust, lb_f
u	= axial component of station velocity, ft/s
UAS	= unmanned aerial system
V	= velocity, ft/s
v	= tangential component of station velocity, ft/s
W	= resultant velocity, ft/s
W_a	= axial velocity, ft/s
W_t	= tangential velocity, ft/s
x	= distance along the chord
y	= vertical distance

Greek

α	= angle of attack or blade incidence angle of flow, deg
β	= angle of blade relative to circumferential or tangential, deg
η	= blade efficiency of each element
η_o	= overall system efficiency
θ	= induced angle given by the difference between the two resultant flow angles, deg
ρ	= density of air, lb_m/ft^3
ϕ	= resultant flow angle with respect to the plane of rotation, deg
Ω	= propeller rotational speed, rad/s

Subscripts

$1, 2, 3, 4$	= axial stations
0.75	= arbitrary ACC radial location of propeller blade quantities
a	= axial
o	= original value
t	= tangential

I. Introduction

THE importance of the Unmanned Aerial System (UAS) is increasing as more tasks are being assigned to these vehicles. The term UAS highlights the systems nature of the vehicle to include the unmanned aircraft, propulsions system, control system and communications or telemetry link. Each is designed to support a particular mission. Since a majority of these vehicles are used for intelligence, surveillance, and reconnaissance (ISR), sensors are an important part of the system. Regardless of the mission and propulsion system, the customer always desires additional sensor capability and/or to remain on station for the longest possible period of time. This results in a tradeoff as the UAS has a limited amount of internal power from which to draw for its mission. If the propulsion system is more efficient, less power would be required for flight allowing for a longer endurance time. Thus, the guiding principle for this research effort is to examine an existing propulsion system for a current UAS and to seek ways to improve both the propulsive efficiency and decrease noise. This paper will examine an improved method to design and test propellers for small UASs. A discussion of propeller design theories will lead to an overview of open-source software available for propeller design. Next BEARCONTROL, an integrated software program developed by the authors, will be discussed leading to a propeller being designed, tested, and compared with a commercial propeller operating at the same conditions.

A. Actuator Disk Theory (Linear Momentum)

A typical open propeller propulsive system for a small UAS employs the power from a battery to drive a propeller that adds mechanical energy to the flow of air through the propeller, increasing the air velocity, to produce thrust. The propeller has an airfoil cross-section that typically varies in blade angle and chord length in the radial direction. As the motor spins, the propeller draws air in from a freestream area, A_1 , to the face of the propeller with a smaller area, A_2 , as is seen in Fig. 1. The propeller adds mechanical power to the flow which directly increases the

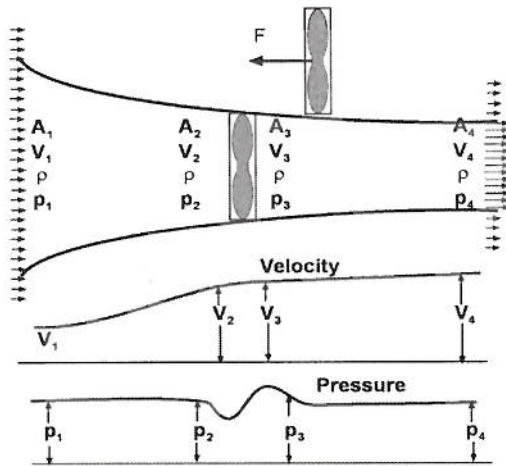


Figure 1. Open propeller depiction of the flow areas occupied by the flow passing through the propeller as well as changes in velocity and pressure in axial relation to the propeller inlets.¹

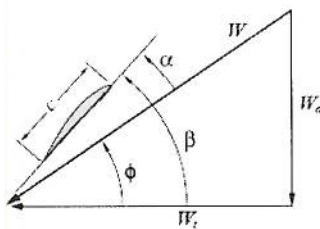


Figure 2. Airfoil cross-section geometric properties.³

designing the blade. It is worth noting that because this theory does not account for induced velocities at the blade, it is assumed that the c_l and c_d data for each element's resultant velocity based on freestream conditions is sufficient for acceptable results. For small UASs, propeller performance depends on having accurate airfoil data, however, limited airfoil data at low Reynolds numbers are available. For small-scale propellers with low chord-based Reynolds numbers, airfoil performance can change significantly with radial location.²

Figure 2 shows an airfoil cross-section with a chord length of c , at a radial coordinate r , along a propeller blade with a tip radius of R . The cross-section experiences a resultant velocity, W , that is composed of W_a , the axial velocity, and W_t , the tangential velocity. In this theory, the axial velocity represents the forward speed of the propeller, or the flight speed. The tangential velocity represents the velocity seen by the propeller due to rotation. The velocity near the hub is much less than that of the velocity at the tip of the propeller. This can be seen by the relation shown in Eq. (1)

$$W_t = \Omega r = 2\pi nr \quad (1)$$

where Ω is the angular velocity of the propeller in radians per second and n is the rotational velocity in cycles per second. The remaining parameters are β , the geometric pitch of the cross-section with respect to the plane of rotation, ϕ , the resultant flow angle with respect to the plane of rotation, and α , the airfoil cross-section angle of attack, which is measured from the resultant velocity vector, W .

static pressure of the flow stream. The higher static pressure then decreases to ambient or atmospheric pressure, thus, increasing the velocity and further reducing the throughflow area to A_4 . The propeller's interaction with the oncoming flow and the size of flow areas result in the thrust used to propel the vehicle.

Propellers are extremely difficult to analyze because (1) the tangential velocity of the propeller blades increases with radial position, (2) the axial velocity of the flow approaching the propeller blades increases from the freestream velocity as the propeller thrust increases, (3) the geometry of the propeller blades (i.e. chord and angle of twist) depends upon radial location, and (4) the Reynolds number is relatively small (especially near the hub) and depends on radial location and chord length. Thus, additional methods are required to more accurately design and predict propeller performance.

B. Blade Element Theory

Because linear momentum theory does not account for blade geometry, Blade Element Theory (BET) was developed. BET divides the blades of the propeller into individual airfoil cross-section elements which are analyzed based on the local, two-dimensional velocities seen at each location. After analyzing the flow over each element, the resulting forces can be determined. A final integration over the entire blade will give the performance characteristics. This theory allows for the analysis of specific propellers with radially varying geometric shapes. While BET is more detailed than the one-dimensional theory, it does not account for induced velocities at the blades, swirl in the slipstream, non-uniform flow, or propeller blockage. This analysis requires the knowledge of the aerodynamic properties of the airfoil cross-section(s) in use when

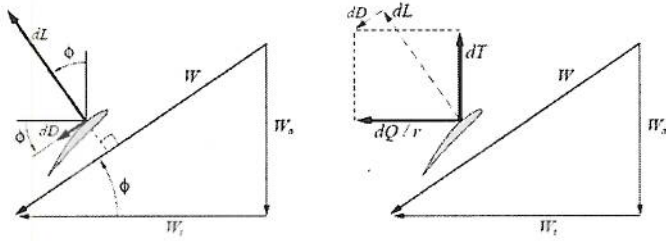


Figure 3. Decomposition of Lift and Drag into Thrust and Torque.³

It is also important to visualize how the components of lift and drag for an airfoil section are resolved into thrust and torque, as seen in Fig. 3. Components of these lift and drag vectors may be taken in order to calculate information more relevant to propellers such as the elemental thrust and torque, or dT and dQ/r , for each section. It can be seen that the elemental thrust may be computed with

$$dT = dL \cos \Phi - dD \sin \Phi = \frac{1}{2} \rho W^2 c dr (c_l \cos \Phi - c_d \sin \Phi) \quad (2)$$

where dr is the elemental width of the airfoil cross-section. Similarly, it can be seen that the elemental torque may be described by

$$dQ = (dL \sin \Phi + dD \cos \Phi) r = \frac{1}{2} \rho W^2 c r dr (c_l \sin \Phi + c_d \cos \Phi) \quad (3)$$

With the definitions of dT and dQ/r , the blade efficiency of each element can be calculated as

$$\eta = \frac{W dT}{\Omega dQ} = \frac{W(c_l \cos \Phi - c_d \sin \Phi)}{\Omega r (c_l \sin \Phi + c_d \cos \Phi)} = \tan \Phi \frac{c_l \cos \Phi - c_d \sin \Phi}{c_l \sin \Phi + c_d \cos \Phi} \quad (4)$$

An integration over each blade must now be performed in order to determine the total thrust, torque, and efficiency of the propeller. In order to do so, the aerodynamic characteristics at each cross-section across the blade must be known—these change when moving outward to the blade tip due to the change in W_t as shown in Eq. (1). Once this data are known, Eqs. (5) through (7) may be used to determine the thrust, torque, and overall efficiency of the propeller

$$T = \int_0^R dT = \frac{1}{2} \rho B \int_0^R W^2 c (c_l \cos \Phi - c_d \sin \Phi) dr \quad (5)$$

$$Q = \int_0^R dQ = \frac{1}{2} \rho B \int_0^R W^2 c r (c_l \sin \Phi + c_d \cos \Phi) dr \quad (6)$$

$$\eta_o = \frac{\int_0^R W dT}{\Omega \int_0^R dQ} \quad (7)$$

where the density is considered incompressible and B represents the number of blades on the propeller.

C. Blade Element Momentum Theory

Blade Element Momentum Theory (BEMT) includes the torque imparted by the rotor on the fluid or swirl and accounts for induced velocities created by the production of lift on each propeller blade. It is necessary to know these velocities to determine the appropriate twist of the blade. These induced velocities of the propeller blades can be calculated and incorporated into propeller performance predictions. The main assumption that is limiting this theory's prediction capability is that the flow over the elemental airfoil cross-sections is only two dimensions.

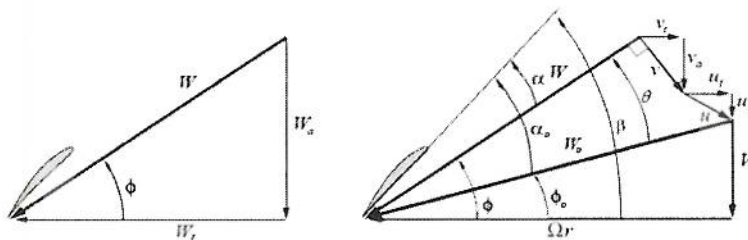


Figure 4. Velocity decomposition and angle definitions.³

be calculated and incorporated into propeller performance predictions. The main assumption that is limiting this theory's prediction capability is that the flow over the elemental airfoil cross-sections is only two dimensions.

Figure 4 shows the velocity decomposition of the resultant velocity, W . The total axial velocity, W_a , is composed of the

flight velocity of the vehicle, V , and induced velocities v_a and u_a . The total tangential velocity seen by the propeller, W_t , is composed of the rotational speed of the propeller, Ωr , and induced velocities v_t and u_t . The induced velocities v_a and v_t are a product of the lift produced by the propeller blade and are generally positive for a propeller that is producing positive thrust. The induced velocities u_a and u_t are included in the decomposition to describe externally-induced velocities. For the purposes of this work, these will be assumed to be zero. Velocity components with a "o" subscript are the original velocity components discussed in the BET section. W_o is the original resultant velocity composed of the flight velocity of the vehicle, V , and the rotational velocity of the propeller, Ωr .

Figure 4 also defines the angles that will be used in the BEMT analysis. The geometric pitch of the blade section is given by β . Variables with an "o" subscript designate angles associated with the velocity vectors discussed when referring to BET. Those without the subscript are associated with the velocity components that account for the previously defined induced velocities. The following relations define the remaining angles in the figure

$$\alpha = \beta - \Phi \quad (8)$$

$$\alpha_o = \beta - \Phi_o \quad (9)$$

$$\theta = \Phi - \Phi_o \quad (10)$$

where α is the angle of attack and Φ the resultant flow angle when induced velocities are accounted for, α_o is the angle of attack and Φ_o the resultant flow angle when induced velocities are not accounted for, and θ is the induced angle given by the difference of the two resultant flow angles.

The definition of elemental thrust for a B -bladed propeller is

$$BdT = B dL \cos\Phi = \frac{1}{2} B c_l W^2 c dr \cos\Phi \quad (11)$$

From Fig. 4, it can also be discerned that the induced velocity component in the thrust direction is given as

$$v_a = v \cos\Phi \quad (12)$$

which, when coupled with momentum theory, where $dA = 2\pi r dr$, can show that the total elemental thrust for a B -bladed propeller may also be written as

$$BdT = \rho(2\pi r dr)(V + v \cos\Phi)(2v \cos\Phi) \quad (13)$$

If Eqs. (11) and (13) are equated, a definition for the induced velocity, v , may be found:

$$v = \frac{B c_l c W^2}{8 \pi r (V + v \cos\Phi)} \quad (14)$$

Equation (15) is derived from Fig. 4 and is used to obtain the elemental thrust and torque—Eqs. (16) and (17), respectively.

$$W = W_o \cos\theta = \left(\frac{2\pi nr}{\cos\Phi_o} \right) \cos\theta \quad (15)$$

$$\begin{aligned} dT &= B(dL \cos\Phi - dD \sin\Phi) = \frac{1}{2} B \rho W^2 c dr (c_l \cos\Phi - c_d \sin\Phi) = \\ & B \rho \left(\frac{2\pi nr}{\cos\Phi} \cos\theta \right)^2 c dr (c_l \cos\Phi - c_d \sin\Phi) \end{aligned} \quad (16)$$

$$\begin{aligned} dQ &= B(dL \sin\Phi + dD \cos\Phi) = \frac{1}{2} B \rho W^2 c r dr (c_l \sin\Phi + c_d \cos\Phi) = \\ & B \rho \left(\frac{2\pi nr}{\cos\Phi} \cos\theta \right)^2 c r dr (c_l \sin\Phi + c_d \cos\Phi) \end{aligned} \quad (17)$$

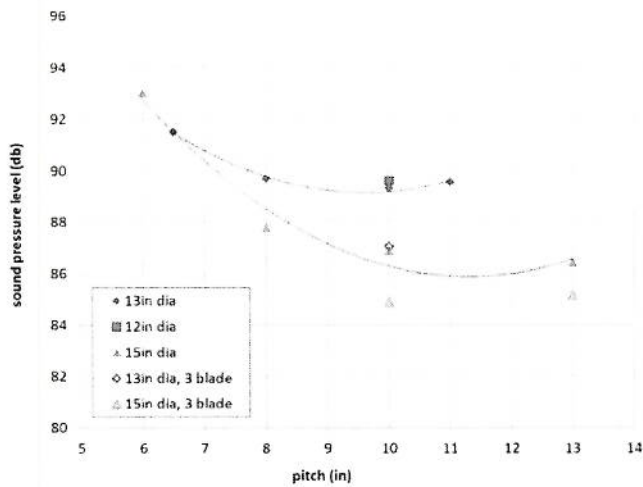


Figure 5. SPL as a function of pitch for 12 ACC propellers producing 2.5 lbf of thrust at 44 ft/s freestream velocity.⁴

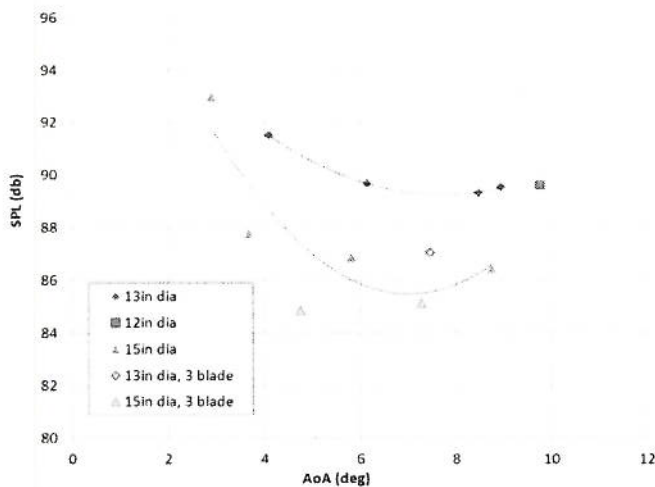


Figure 6. SPL as a function of propeller angle of attack α at $r = 0.75R$ for 12 ACC propellers producing 2.5 lbf of thrust at 44 ft/s freestream velocity.⁴

D. Importance of airfoil data in propeller design

Fig. 5 shows the sound pressure level (SPL) as a function of propeller pitch with data taken at the USAF Academy for commercial aero-nautCAMcarbon (ACC) folding propellers.⁴ The 13 and 15 in propeller data appear to suggest optimal pitches for these operating conditions that will minimize sound pressure level.

Figure 6 shows SPL plotted as a function of the propeller angle of attack at $r_{0.75}$ for 12 propeller configurations. The angle of attack is determined using the velocity triangles outlined previously (Fig. 2). The minimum SPL for 13 and 15 in diameter propellers appear to line up at an angle of attack between 7 to 8 degrees. This angle of attack closely corresponds to the location of maximum c_l/c_d for the Clark Y airfoil. This airfoil is widely used as a cross-section for commercial propellers and is likely the airfoil used for this propeller family. The minimum SPL for a particular angle of attack indicates the importance of selecting the proper pitch and diameter to match the operating conditions so that the propeller is performing at the optimal angle of attack to maximize c_l/c_d and minimize SPL. Ensuring that this angle of attack is maintained over the entire span of the propeller is therefore critical in the design of custom propellers.

II. Propeller Design And Fabrication

Several low or no cost propeller/wind turbine software design programs were investigated for this study. A summary of the programs are listed, reflecting the experiences of the authors:

PROP-DESIGN⁵: This program is an open source, public domain, aircraft propeller design software. It is targeted for aircraft straight/swept, constant/elliptical chord propellers from Mach 0 to 1.3. It uses vortex theory. While PC based, the program runs in the Command Prompt window and is not suited for model aircraft sized propellers.

PROPID⁶: This program, from University of Illinois, Urbana Champaign (UIUC), is primarily used for the design and analysis of horizontal axis wind turbines using BEMT. It was not useful for the purposes of designing small propellers.

PROGEN⁷: This program is a wind turbine, power turbine, and propeller design program used to design in an arbitrary fluid or gas. The program was difficult to install and was too simplistic for the required purpose.

OPENPROP⁸: This is software for designing optimized marine propulsors or horizontal axis turbines and is not suited for the design of small propellers. It runs using MATLAB.

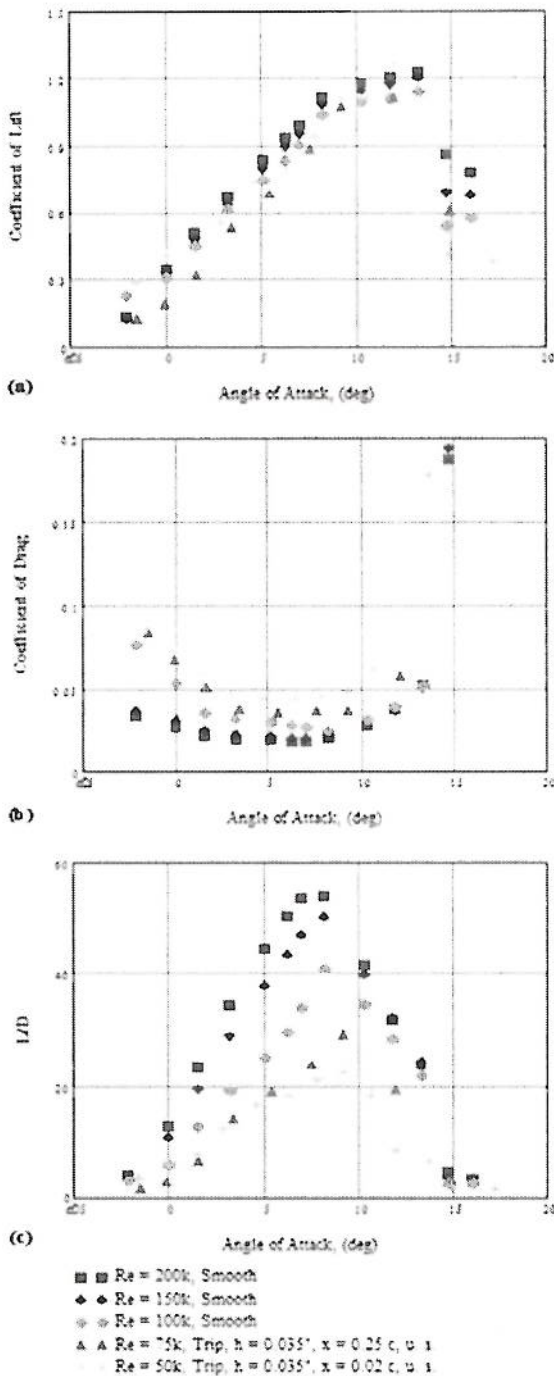


Figure 7. S823 airfoil data for low Reynolds numbers.¹³

separation which can reduce the thrust of the propeller thereby reducing the efficiency. Burdett et al. studied an airfoil under these low flow conditions and found it necessary to trip the boundary layer to turbulent flow for Reynolds numbers under 100,000.¹³ Also noted by Burdett et al. was the dependence of the angle of attack for optimum lift to drag ratio changes with Reynolds number, as shown in Fig. 7c. As the Reynolds number increases,

PROPDESIGNER⁹: PropDesigner is a program to investigate propeller design based on combined blade and momentum theory. It allows the design and analysis of propellers both on and off the design points. It has limited airfoil availability. The program would not install properly on local computers.

LOCALLY DEVELOPED SPREADSHEET¹⁰: This spreadsheet, developed by the authors, designs a propeller analytically using BEMT however it does not interface with a CAD program for propeller prototyping.

J-BLADE¹¹: This program is an open-source propeller design and analysis code using BEMT. It incorporates other open source codes, in particular Q-Blade a wind turbine design program, to estimate propeller performance. While this code shows promise, it does not interface with computer solid modeling software.

JAVAPROP¹²: This is a propeller design and analysis software package based on blade element theory which can be run off the internet or on a local PC. It is menu driven with a GUI and has user friendly interfaces. It uses Reynolds number dependent airfoil data and has an output format compatible with CAD programs. Because of its simplicity and ease of use this software package was used for the initial design of propellers for this study however, it was not useful enough for long term.

QMIL/QPROP³ QPROP is an analysis program for predicting performance of propeller-motor combinations. QMIL is a companion propeller design program. The aerodynamic models used in QPROP account for induced velocities and are very complete. Also included is a basic motor model which is useful to model the UAS propulsion system. This computer model served as the basis for the propeller design program developed by the authors.

During the design process it was noticed that the local Reynolds numbers over the span of the propeller were below 100,000 and typically were below 50,000. For these ranges of Reynolds numbers the flow over the propeller blade is susceptible to flow

the optimum angle of attack decreases. This is important information for optimizing the design of propellers using the BEMT. Burdett tested 2-D airfoils in a wind tunnel under low Reynolds number conditions. Wind tunnel data are not always available and wind tunnel testing is not always practical. An alternative is to use one of several programs to generate airfoil data. The following are a list of software programs investigated:

JAVAFOIL¹⁴: A companion program to JAVAPROP for the analysis of airfoils. This program is menu driven and simple to use however, no method of creating or importing lift and drag coefficients was readily available so this program was not pursued.

XFLR5¹⁵: This program is an analysis tool for airfoils, wings and planes operating at low Reynolds numbers. It uses a program called XFOIL to calculate lift and drag coefficients. While this program was an excellent program, it was too broad in its application for the design of propellers.

XFOIL¹⁶: This is a menu driven program for the design and analysis of subsonic isolated airfoils. It enables a particular airfoil to be entered into the program and then lift and drag coefficients are calculated using a panel method. It also allows for the boundary layer to be tripped at locations over the surface of the airfoil which is useful information for low Reynolds numbers where the flow will be separated. This software was used to determine the angle of attack for the optimum (maximum) lift to drag ratio at a given Reynolds number when actual data are not available.

III. Noise Generation

Of importance in the design of a propeller is the generation of noise. Noise must be minimized and the most direct improvement for lowering noise is reducing the RPM. Figure 8 shows that the noise intensity of the propeller and test stand under the conditions of 2.5 lbf of thrust at 44 ft/s freestream velocity. More needs to be accomplished with noise testing to verify noise levels of the propeller. Figure 8 clearly shows that reducing the RPM is one desirable method for reducing noise.

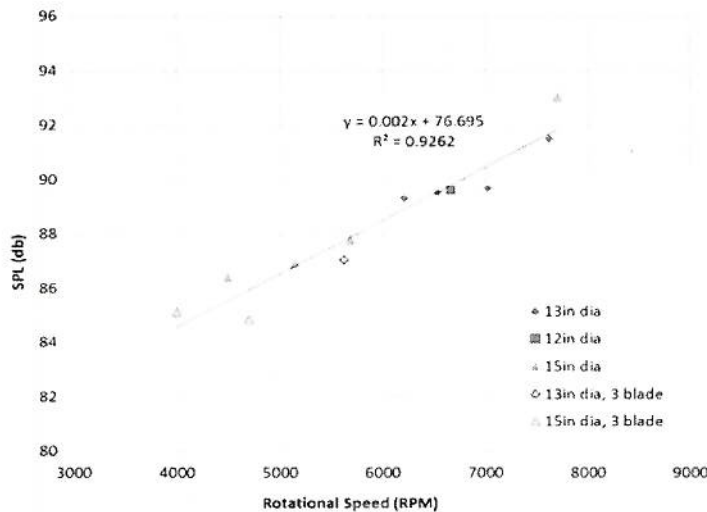


Figure 8. SPL as a function of propeller rotational speed for 12 ACC propellers while producing 2.5 lbf of thrust at 44 ft/s freestream velocity.⁴

IV. BEARCONTROL

BEARCONTROL is a MATLAB code that has drastically reduced the time required for propeller design, analysis, solid-modeling, and in turn, fabrication of the propellers experimentally tested in this work. In general, this program enables a user the ability to start the design of a propeller and have the rapid-prototyped model in as short a time as a single day. BEARCONTROL accomplishes this task by providing a single platform for a user to control multiple programs at once. The programs handled by BEARCONTROL are QMIL for the propeller design, QPROP for the motor and propeller performance analysis, NAFNoise for the propeller noise prediction, and SolidWorks for the solid-modeling. The following list gives additional detail of each program's background and capabilities.

- QMIL—the first of two command prompt programs in a propeller design and analysis package developed by Drela.³ This program designs a propeller geometry based on physical and design point operation constraints using the BEMT. The output is conveniently the input for the propeller analysis program QPROP.
- QPROP—the second of the two command prompt programs developed by Drela.³ This program analyzes the geometric design from QMIL using the BEMT - QMIL and QPROP formulations are perfectly

consistent with each other. It is possible for QPROP to analyze propeller designs not created by QMIL as long as the designs are entered into QPROP in the correct format.

- NAFNoise—an airfoil noise prediction command prompt program developed by NREL. This program predicts the noise of individual airfoils.¹⁷
- SolidWorks—the 3D CAD program created by DASSAULT SYSTEMS. BEARCONTROL creates solid-modeling macros for use in the SolidWorks Application Programming Interface (API) to automate the creation of the propeller 3D models.¹⁸

BEARCONTROL employs these programs to create a useful and comprehensive propeller production tool that has dramatically decreased propeller manufacturing time, and in turn, has increased propeller testing capabilities in this project. A user guide for BEARCONTROL is available.¹⁹

A. MATLAB GUI

The governing code that controls all programs is written in the versatile programming language, MATLAB. It produces a graphical user interface (GUI) (Fig. 9) which allows a user to indirectly control the subsidiary programs without having to learn the input and/or coding protocols pertaining to each one.

The GUI contains input boxes for all of the necessary data in order to run QMIL, QPROP, NAFNoise, and to produce Visual Basic (VBA) code used to automatically model the propeller in SolidWorks. Figure 10 is a flow chart which depicts a typical session of BEARCONTROL. Intermediate inputs that are necessary to run these programs are created “behind the scenes” in the MATLAB code based on user inputs and program outputs that the individual codes may produce during each run of BEARCONTROL.

The process begins with user inputs of all necessary data to complete a propeller design, analysis, noise prediction, and to create the solid-modeling macros. BEARCONTROL will then create an input file and run the propeller design program QMIL. Upon completion, QMIL outputs the propeller geometry file which conveniently becomes the input to the propeller analysis program, QPROP. Once BEARCONTROL runs QPROP to analyze the propeller, it moves on to the noise calculation in the code. If the user selected the option to predict noise, then BEARCONTROL will run NAFNoise for each BEMT blade section of the propeller design to predict their

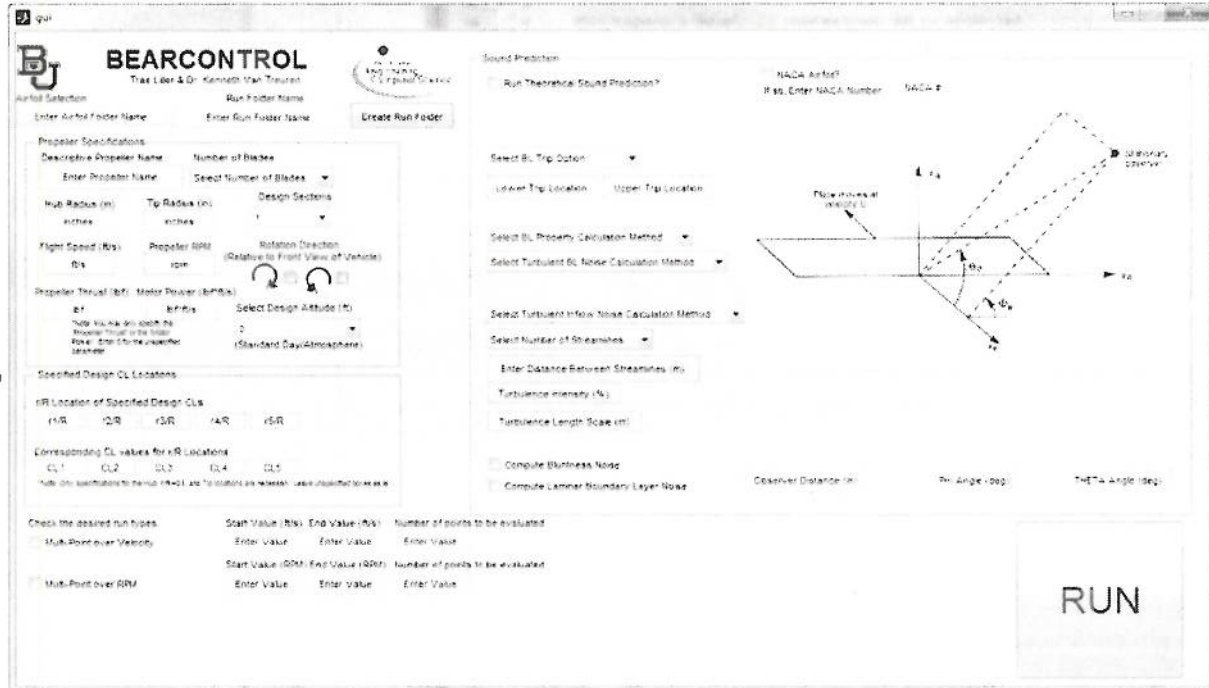


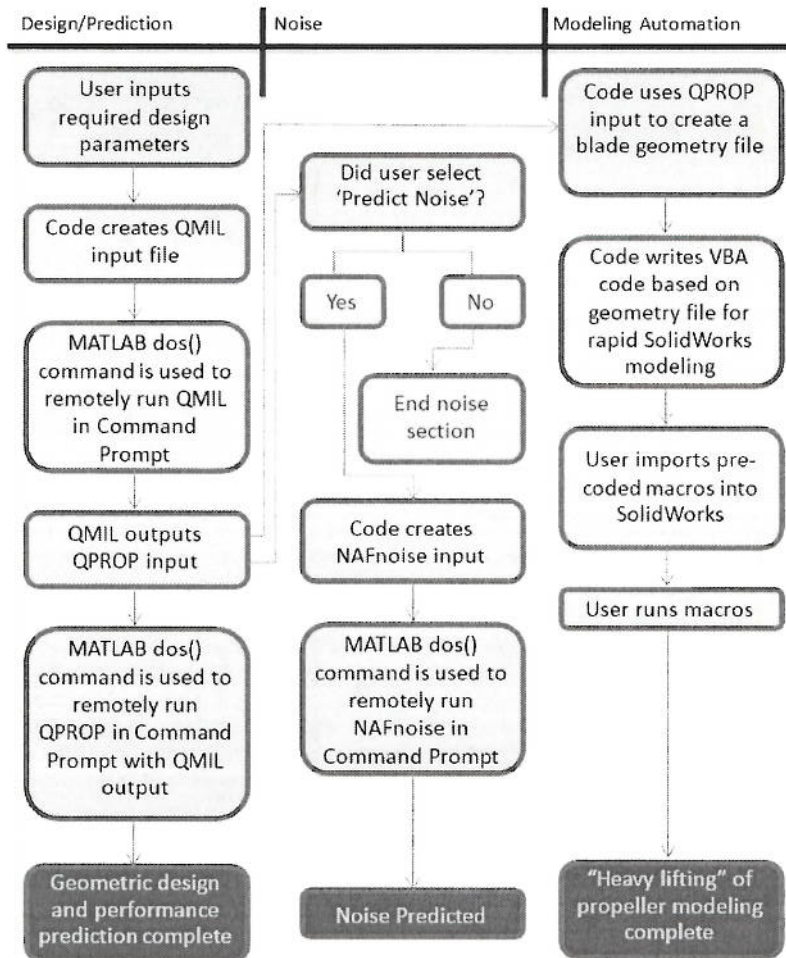
Figure 9. BEARCONTROL GUI.

individual noise signatures, and then sum the noise signatures across each blade to produce a total blade noise prediction. Finally, BEARCONTROL will create a geometry file formatted specifically for the SolidWorks macros based on the propeller geometry design output from QMIL and the specified airfoil shape chosen by the user. The last step the code will perform is to pre-code VBA macros that will automatically place reference planes for each airfoil section and insert the splined airfoils to their respective reference planes. A typical result of the macros can be seen in Fig. 11.

A supplement to the QPROP code was the code, "constantchordhelper.m" designed to achieve a constant chord or flat tip design. The thrust production distribution across the blade for this constant chord propeller would ultimately lead to a smaller chord near the hub, eliminating issues with the blade to hub connection modeling in SolidWorks. It would also produce more thrust in the outer regions of the blade, limiting the effect of any flow interaction with the test stand to regions of the blade that produce less thrust.

B. The Propeller Noise Prediction Subroutine

Although the NAFNoise subroutine has not been finally implemented, it is a feature of BEARCONTROL that will become important in future research. This subroutine requires the inputs stated in the "Sound Prediction" box of BEARCONTROL as well as the QMIL output and a text file with the coordinates of the airfoil being used. These inputs, the QMIL output, and the airfoil geometry coordinate file allow BEARCONTROL to create NAF Noise input files. Any inputs needed that are not specified from the user in the GUI are calculated or read in from the QMIL or airfoil geometry files.



The output file gives data in columns for each noise source in dB across the given range of frequencies along with a total for each noise source at each frequency. Once all of the blade section noise predictions have been made, BEARCONTROL will sum the total noise of each blade, and then sum the total noise of all blades giving a total propeller noise prediction.

C. Solid-Modeling Automation Subroutine

The solid-modeling subroutine in BEARCONTROL creates run-specific, pre-coded macros for a user to import into SolidWorks to automatically model the majority of the propeller. The only input required from the user is the airfoil geometry coordinate file which is also an input for the noise subroutine. BEARCONTROL will use this along with the QMIL output file in order to create three files. First, BEARCONTROL will create a master geometry file

Figure 10. BEARCONTROL Execution Flow Chart.

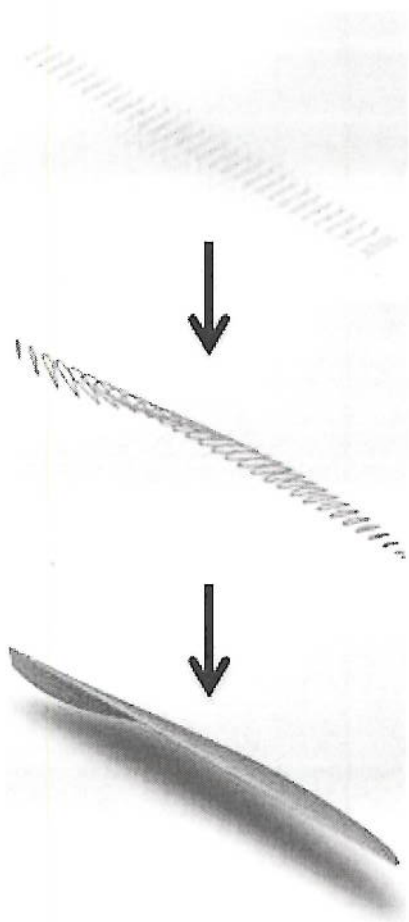


Figure 11: Solid-modeling Macro Output, a) reference planes for each airfoil section, b) each splined airfoil section at designed geometric pitch on its designated reference plane, and c) the solid model.



Figure 12. Baylor University Subsonic Wind Tunnel.

that contains the coordinates for every airfoil section in the blade design from the QMIL output. This is accomplished by reading the geometry specifications (radial location, chord, and geometric pitch angle) from the QMIL output and applying necessary mathematical operations to the normalized airfoil geometry coordinate file to have the points represent the design for every radial section. The points for each airfoil are concatenated in a single file that will be read later as needed. Next, BEARCONTROL pre-codes the “plane macro,” which will insert reference planes in to SolidWorks with respect to each radial design location from the QMIL output file. Finally, a “spline macro” is created which will insert the airfoil point data already splined together on each reference plane as dictated by the geometric design of the propeller. Typical outputs of these two macros can be seen in Fig. 13.

E. Experimental Propeller Testing Facility

Propeller experiments took place in the Baylor University Subsonic Wind Tunnel (Fig. 12) which is an Engineering Laboratory Design, Inc. Model 406B. The open loop tunnel is capable of achieving wind speeds of up to 165 ft/s. These speeds are attained through a constant-pitch fan driven by a variable-speed, 40-hp motor. At the inlet of the 4 ft long and 2 ft square test section, the velocity variation is $\pm 1\%$ and the turbulence intensity is less than 0.2%. Figure 13 shows the propeller test stand and its components.

The instruments/components are as follows:

1. Transducer Techniques LSP-1 Load Cell—used to directly measure the thrust of the propeller. Has a maximum load capacity of approximately 2.2 lb_f.
2. Interface MRT-0.2NM Torque Transducer—used to directly measure the torque of the propeller. Has a maximum load capacity of approximately 1.77 in-lb_f.
3. Custom 3-D Printed Motor Housing—houses and connects the motor to the torque transducer.
4. APC 9x6 Propeller—base propeller for testing.
5. Undisclosed UAS Motor—motor supplied for testing.
6. Omega HHT20-ROS Remote Optical Sensor—used to count the rotations of the propeller during experimental operation. Has a speed range of 1-250,000 RPM.
7. In-tunnel Brüel & Kjær 4938-A-011 ¼” Pressure Field Microphone with Wind Screen
8. Tunnel Inlet Brüel & Kjær 4938-A-011 ¼” Pressure Field Microphone

An uncertainty analysis was accomplished using the method according to Kline and McClintock.²⁰ This resulted in an uncertainty in thrust of ± 0.0008 lb_f, in RPM of ± 0.333 RPM, in freestream velocity of ± 0.0026 ft/s, in overall efficiency of $\pm 0.0011\%$, in SPL of ± 0.2 dB, and a torque uncertainty of ± 0.0011 in-lb_f.

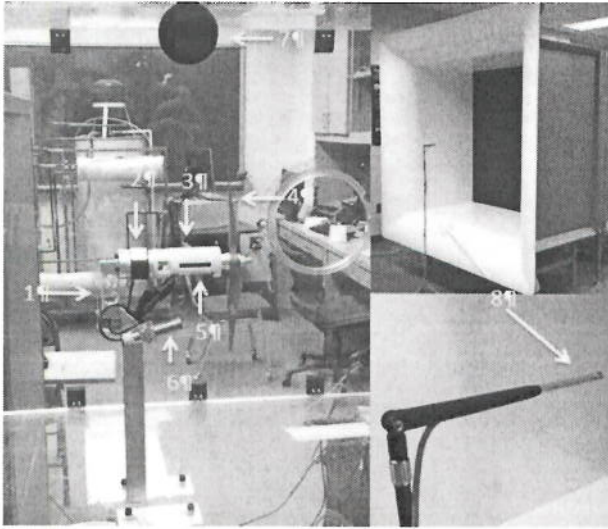


Figure 13. Propeller Test Stand.

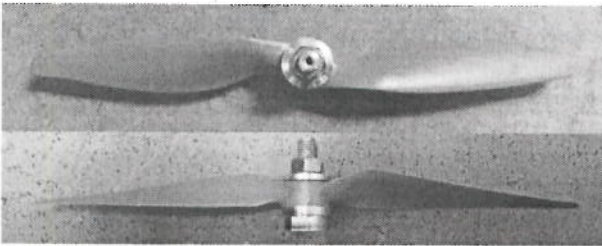


Figure 14. UAS Commercial Propeller: APC 9x6.

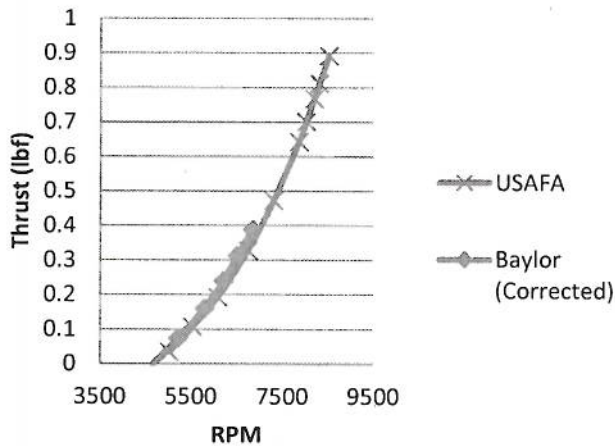


Figure 15. Testing APC 9x6 propeller at the USAF Academy and Baylor University, Thrust vs. RPM.

F. Testing and Comparison of Propellers

The motivation for this study was to test a commercial propeller currently used on a UAS and then to design a propeller that would be more efficient and produce less noise. The commercial propeller was an Advanced Precision Composites (APC) 9x6 which is shown in Fig. 14. This propeller was tested both at Baylor University and the USAF Academy with the results shown in Figs. 15, 16, and 17. The design point used for testing was 0.5 lbf of thrust at a freestream velocity of 44 ft/s. Standard Glauret corrections for the confined streamtube were applied to the data. The graphs also show a correction for density. When accounting for the density differences and examining the thrust and torque plots, both facilities are operating in a similar manner. Agreement is very good between the facilities. The graphs show the sensitivity of the measurements when considering efficiency. Due to power supply limitations, the Baylor data was only able to reach the design point thrust for this series of tests.

Next a propeller was designed using BEARCONTROL and the research experience gained from testing at the USAF Academy.²¹ This led to the design of a constant chord propeller with an oval tip shown in Fig. 18. Design point specifications are given in Table 1. It was important to find an airfoil which would provide good aerodynamic characteristics as well as be structurally strong to provide the stiffness necessary for testing. If the airfoil cross-section is too thin then there would be bending and twisting of the propeller under load. The airfoil used was chosen from the University of Illinois Urbana-Champaign data base.²² The S4233 airfoil had available data for in the Reynolds number range needed, 60,200. The airfoil cross-section can be seen in Fig. 19. The lift and drag provided an L/D_{max} of 32.4, shown in Fig. 20, at an angle of attack of 8.23°. The design RPM of 4000 was chosen to reduce the noise signature and, since the propeller was designed to produce 0.5 lbf of thrust, this lower RPM and increased the chord of the propeller resulting in a stronger structure. The propeller was designed, printed and ready to test in 12 hours using BEARCONTROL. The pressure side of the propeller was painted with black paint to improve the operation of the optical sensor.

Table 1. TPX Design Point Specifications.

Number of Blades	2
Airfoil	S4233
Operating Point Angle of Attack	8.23 degrees
Hub Radius	0.875 inches
Tip Radius	4.5 inches
Flight Speed	44 ft/s
RPM	4000
Thrust	0.5 lbf
Design Sections	35

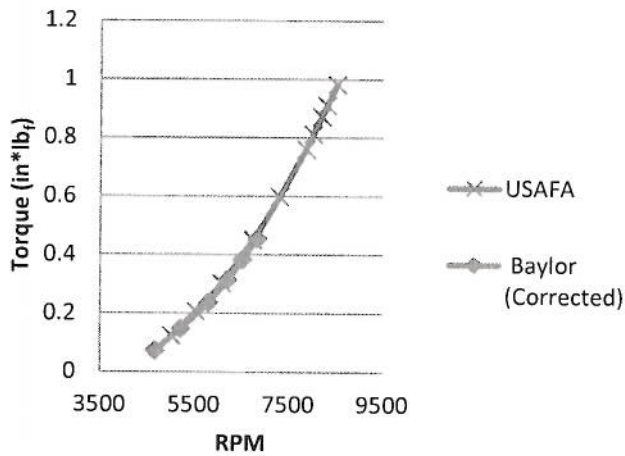


Figure 16. Comparison of Torque for APC 9x6 propeller at V=44 ft/s.

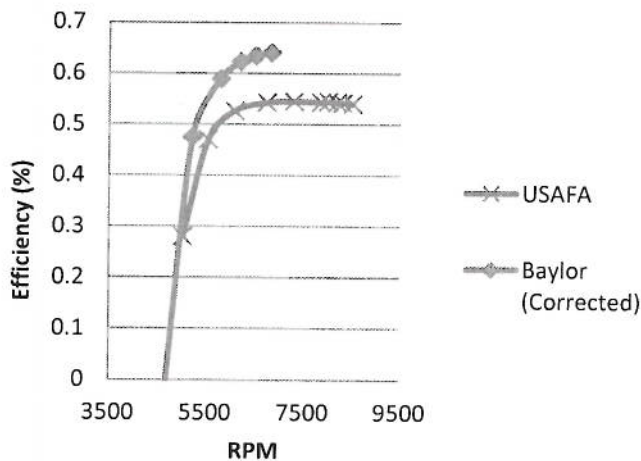


Figure 17. Comparison of Overall Efficiency for APC 9x6 propeller at V=44 ft/s

Testing results are shown in Fig. 21. It is clear that both propellers provide the required operational thrust of 0.5 lbf however this is accomplished at a much lower RPM for the TPX propeller, approximately 2000 RPM lower. Two microphones provided a means to compare SPL at two locations. One microphone, Channel 1, is placed in the tunnel 5.9" above the propeller tip, and 2" downstream of the propeller along the centerline of the wind tunnel. Channel 2 is positioned on a stand in front of the wind tunnel at the inlet to the bellmouth, representing an upwind microphone. The results for Channel 1 in Fig. 22 clearly show that the TPX propeller, operating at a lower RPM, leads to a reduction in the SPL. For Channel 1, this translates to a 1-1.5 dB drop over the range of operation of the propeller, including the design point.

For Channel 2 (Fig. 23), the TPX and APC propeller SPLs diverge with increasing thrust with the difference being approximately 3.5 dB at 0.5 lbf of thrust. Studies have been accomplished at the USAF Academy using a different commercial propeller.²⁰ They found that increasing the number of blades further reduces the RPM and noise of the propeller when designed for a specific operating point. The results of comparing a two bladed commercial propeller with a BEARCONTROL designed constant chord, five blade propeller with oval tips show a reduction in SPL of 12 dB and an efficiency increase of 6.2%, both desirable trends.

VI Construction and Materials

The actual structure of the propeller depends on a number of items. First an airfoil design is necessary that has a thicker cross-section. The airfoil data must be available in the Reynolds number ranges that the propeller will experience. Lower RPM also increases the chord of the propeller when designed for a finite thrust. This is also desirable from a noise as well as a structural point.

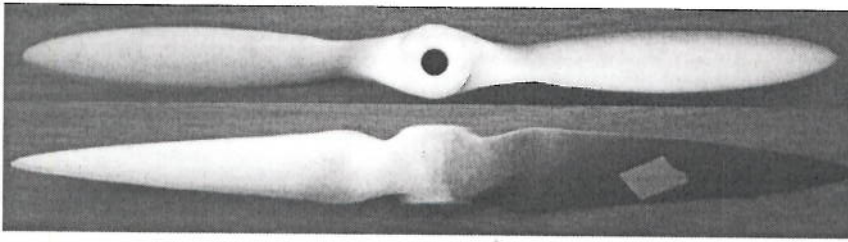


Figure 18 TPX Propeller.

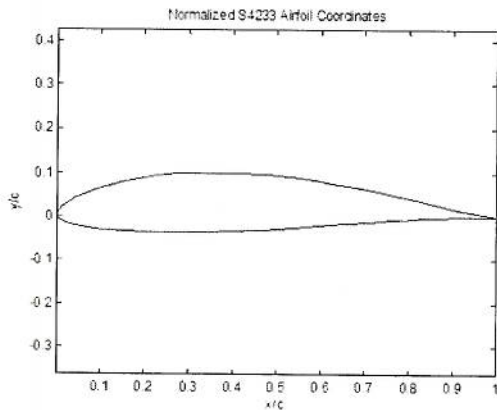


Figure 19. Normalized S4233 Airfoil Cross-section.

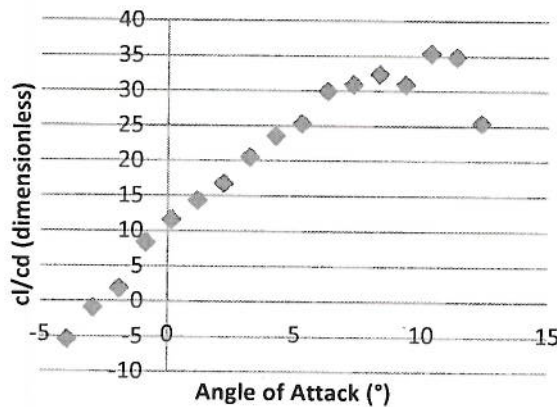


Figure 20. C_l/C_d for the S4233 Airfoil vs Angle of Attack for a Reynolds number of 60,200.

The design of the propellers changed over the testing period. Initially the propellers were printed as one solid propeller oriented on the printer to minimize printing time (see Figure 24). With the number of propellers that were being designed and as the diameter of the propeller

increased, a hub and spoke arrangement was used (see Figure 25). Different hubs were designed to enable testing of multiple blades, up to five. Eventually a more solid hub arrangement was needed as some fatiguing was evident with the material that was being used for the propellers (one of the hubs failed during testing). The final design used an aluminum hub that was hollowed out to achieve a very similar weight as the solid hub used previously. The final arrangement can be seen in Fig. 26. This hub has performed well over the testing period.

The last consideration for the rapid prototyping of propellers is the machine used to print the propellers. For this study an OBJET 30 was used with a VeroWhite ABS material. The objet has a resolution of 0.0039 inches which is sufficient to print the propeller without additional surface finishing. An example of this type of propeller blade can be seen in Figure 18. After several printing sessions it was desired to print the propeller with the hub flush to the surface so that the surface finish will

be similar on the pressure and suction surfaces of the propeller. This minimizes any vibration issues from asymmetric aerodynamic forces which may be occurring on the propeller as a result of the surface finish. Always balance the propellers before testing as well. Another type of rapid prototype machine used was a Viper SI2 SLA System printer from the USAF Academy. This printer had different settings for resolutions which effected the print build size. The SLA printer did require some surface finishing prior to testing. The material used, Accura Xtreme Gray, also was susceptible to fatigue failure which occurred with of one of the hubs. Figures 24 and 25 show the propellers made using the SLA rapid prototype machine.

For building a successful model, it is recommended that the structure is sufficient to alleviate any torsion or bending of the propeller blade, a rapid prototype machine with the best resolution available be used, and that the propeller print orientation promotes as uniform a propeller surface finish as possible.

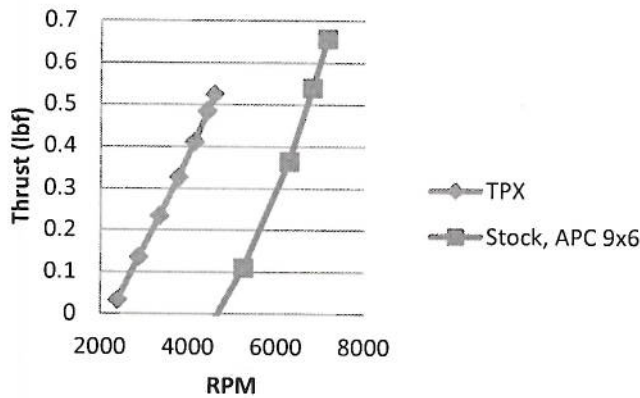


Figure 21. Comparison with TPX and APC 9x6 propeller at $V=44\text{ft/s}$.

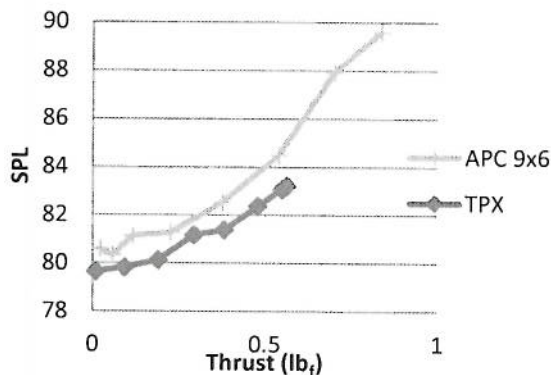


Figure 22. SPL vs Thrust for TPX and APC 9x6 propellers for microphone in the wind tunnel, Channel 1.

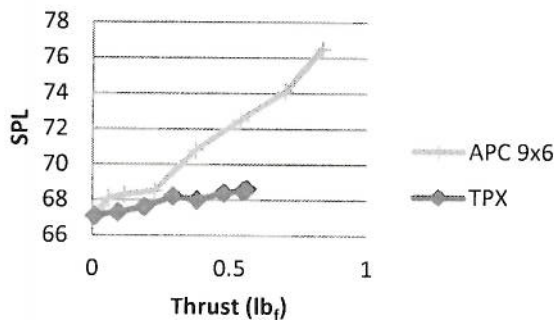


Figure 23. SPL vs Thrust for TPX and APC 9x6 propellers for microphone in front of the wind tunnel, Channel 2.

VII Conclusions

With the importance of UASs in today's society, A procedure has been designed and tested which makes possible the rapid design and manufacture of propellers for testing. BEARCONTROL is a MATLAB GUI that allows the user to input propeller design parameters into the interface screen. With these inputs, the appropriate files are generated to use QMIL and QPROP as well as output geometry files formatted specifically for the SolidWorks macros. With this procedure a propeller can be designed, printed and tested in a matter of hours. In addition to the propeller design process, BEARCONTROL has the ability to use NAFNoise to look at the noise generated across the propeller from the hub to the tip. This allows for a quantitative comparison of the noise generated by the propeller designs. An example of the design process shows that the designed propeller, TPX, was able to reduce the noise signature from the commercial APC propeller by 1-1.5 dB in the wind tunnel and by almost 3.5 dB upstream of the tunnel at the design point. The efficiency of the propeller was reduced from 64.5% for the APC 9x6 propeller to 57.2% for the TPX propeller (an 11.3% reduction) however efficiency can be improved by a more aerodynamically efficient airfoil and better orientation of the propeller on the rapid prototyping machine to achieve a smoother surface on the propeller. A discussion of manufacturing methods concludes that a thicker structure, stiff materials, and the best resolution possible is necessary to have a propeller specimen that will yield quality, repeatable results when testing.

Acknowledgments

The authors would like to thank the United States Special Operations Command for their support of this research. Also, thanks go to the USAF Academy and Baylor University for providing the facilities and resources to accomplish the experimental testing.

References

- ¹"Froude's Propeller Theory". Aerodynamics for Students, Aerospace, Mechanical and Mechatronic Engineering, University of Sydney, 2005.
- ²Burdett, T., Gregg, J., and Van Treuren, K. W., "An Examination of the Effect of Reynolds Number on Airfoil Performance," ESFuelCell2011-54720, *Proceedings of ASME 2011 5th International Conference on Energy Sustainability & 9th Fuel Cell Science, Engineering and Technology Conference ESFuelCell2011*, Washington,

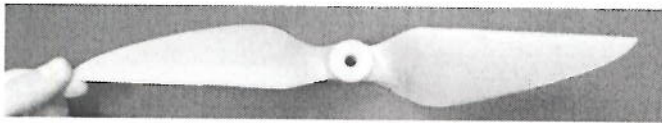


Figure 24. Solid propeller example.

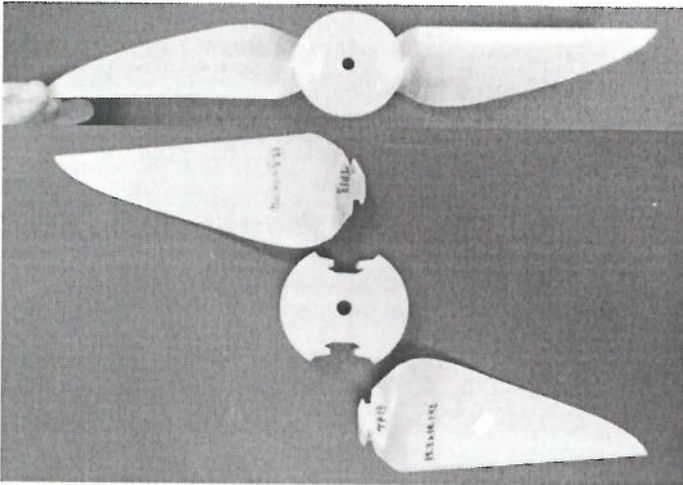


Figure 25. Hub and spoke propeller design.



Figure 26. Aluminum hub design.

accessed on May 12, 2015.

¹³Burdett, T., "Designing a Small-Scale, Stall-Controlled, Horizontal-Axis Wind Turbine," Masters Dissertation, Department of Mechanical Engineering, Baylor University, Waco, TX, May 2012.

¹⁴Hepperle, M., JAVAFOIL, <http://www.mh-aerotoools.de/airfoils/javafoil.htm>, 2003, accessed on May 12, 2015.

¹⁵xflr5, <http://www.xflr5.com/xflr5.htm>, accessed on May 12, 2015.

¹⁶XFOIL, <http://web.mit.edu/drela/Public/web/xfoil/>, accessed on May 12, 2015.

¹⁷Moriarty, P., NREL AirFoil Noise (NAFNoise), NWTC Information Portal (NAFNoise), <https://nwtc.nrel.gov/NAFNoise>, last modified 24-September-2014 ; accessed May 12, 2015.

¹⁸Solidworks, Dassault Systems, <https://www.solidworks.com/>, accessed on May 12, 2015.

¹⁹Liller, W. R., "The Design of Small Propellers Operating at Low Reynolds Numbers and Associated Experimental Evaluation," Masters Dissertation, Department of Mechanical Engineering, Baylor University, Waco, TX, August 2015.

²⁰Kline, J. S., and McClintock, F. A., "Describing Uncertainties in Single-Sample Experiments," *ASME Journal of Mechanical Engineering*, January 1953, pp. 3-8.

²¹Wisniewski, C. F., Byerley, A. R., Heiser, W. H., Van Treuren, K. W., and Liller, W. R., "The Influence of Airfoil Shape, Tip Geometry, Reynolds Number and Chord Length on Small Propeller Performance and Noise," AIAA 33 Applied Aerodynamics Conference, Dallas, TX, June 22-26, 2015.

²²Selig, M., UIUC, Department of Aerospace Engineering, UIUC Airfoil Coordinates Database, http://m-selig.ae.illinois.edu/ads/coord_database.html, accessed on May 12, 2015.

DC, August 7-10, 2011.

³Drela, M., 2006, "QPROP Formulation," <http://web.mit.edu/drela/Public/web/qprop/> accessed on April 29, 2015.

⁴Wisniewski, C. F., Byerley, A. R., Heiser, W. H., Van Treuren, K. W., Liller, W. R., and Wisniewski, N., "Experimental Evaluation of Open Propeller Aerodynamic performance and Aero-acoustic Behavior," AIAA 33 Applied Aerodynamics Conference, Dallas, TX, June 22-26, 2015.

⁵Falzone, A. PROP_DESIGN, <http://propdesign.jimdo.com/> accessed on May 12, 2015.

⁶Selig, M., UIUC, Department of Aerospace Engineering, PROPID, <http://m-selig.ae.illinois.edu/propid.html>, accessed on May 12, 2015.

⁷Vyriotes, P., PROPGEN, <http://www.propgen.com/>, accessed on May 12, 2015.

⁸Epps, B. P., and Kimball, R. W., "OpenProp v3: Open-source software for the design and analysis of marine propellers and horizontal-axis turbines," 2013, <http://engineering.dartmouth.edu/epps/openprop/>, accessed on May 12, 2015.

⁹Whapshott, M., PROPDESIGNER, <http://www.propdesigner.co.uk/html/index.html>, accessed on May 12, 2015.

¹⁰Wisniewski, C. F., USAF Academy, CO, 2014.

¹¹Silvestre, M. A. R., Morgado, J., and Pascoa, J. C., "JBLADE: a Propeller Design and Analysis Code," AIAA2013-4220, *AIAA International Powered Lift Conference*. Los Angeles, California, August 12-14, 2013. doi:10.2514/6.2013-4220.

¹²Hepperle, M., JAVAPROP, <http://www.mh-aerotoools.de/airfoils/javaprop.htm>, 2003,